

---



# DGMamba: Domain Generalization via Generalized State Space Model

---

Shaocong Long<sup>1\*</sup>; Qianyu Zhou<sup>1\*</sup>; Xiangtai Li<sup>2</sup>, Xuequan Lu<sup>3</sup>, Chenhao Ying<sup>1</sup>,  
Yuan Luo<sup>1</sup>, Lizhuang Ma<sup>1</sup>, Shuicheng Yan<sup>2</sup>

<sup>1</sup>Shanghai Jiao Tong University <sup>2</sup>Skywork AI <sup>3</sup>La Trobe University

Code: <https://github.com/longshaocong/DGMamba>

## Abstract

Domain generalization (DG) aims at solving distribution shift problems in various scenes. Existing approaches are based on Convolution Neural Networks (CNNs) or Vision Transformers (ViTs), which suffer from limited receptive fields or quadratic complexities issues. Mamba, as an emerging state space model (SSM), possesses superior linear complexity and global receptive fields. Despite this, it can hardly be applied to DG to address distribution shifts, due to the hidden state issues and inappropriate scan mechanisms. In this paper, we propose a novel framework for DG, named DGMamba, that excels in strong generalizability toward unseen domains and meanwhile has the advantages of global receptive fields, and efficient linear complexity. Our DGMamba comprises two core components: Hidden State Suppressing (HSS) and Semantic-aware Patch refining (SPR). In particular, HSS is introduced to mitigate the influence of hidden states associated with domain-specific features during output prediction. SPR strives to encourage the model to concentrate more on objects rather than context, consisting of two designs: Prior-Free Scanning (PFS), and Domain Context Interchange (DCI). Concretely, PFS aims to shuffle the non-semantic patches within images, creating more flexible and effective sequences from images, and DCI is designed to regularize Mamba with the combination of mismatched non-semantic and semantic information by fusing patches among domains. Extensive experiments on five commonly used DG benchmarks demonstrate that the proposed DGMamba achieves remarkably superior results to state-of-the-art models. The code will be made publicly available.

## 1 Introduction

Humans are easily able to recognize images with domain distribution shifts (such as background changes [4] and various lighting conditions [56]) since the main semantic concepts are consistent. However, this is challenging for multimedia [43, 54, 48, 68, 100, 95, 19, 41, 26, 96] and computer vision systems [53, 15, 3, 27, 28, 93, 94, 59]. One effective approach for eliminating distribution shifts is domain generalization (DG) [45, 89, 20, 5], which attempts to encourage models to focus on semantic factors akin to humans and overlook non-essential features [21, 72, 81, 87, 17, 89, 70, 38].

A large amount of research in DG has concentrated on the design of special modules to acquire robust representation [81, 98, 65, 99, 97, 77], including domain alignment [16, 84, 30, 46], feature contrastive learning [32, 47], and style augmentation [86, 92, 8, 68, 78], and *etc.* Nonetheless, prevailing DG methods heavily rely on CNNs as the backbone to extract latent features, only possessing local receptive fields. As a result, they tend to learn local details and overlook global information, impeding generalization and leading to less-desired performances on unseen domains.

---

\*The first two authors contribute equally to this work.

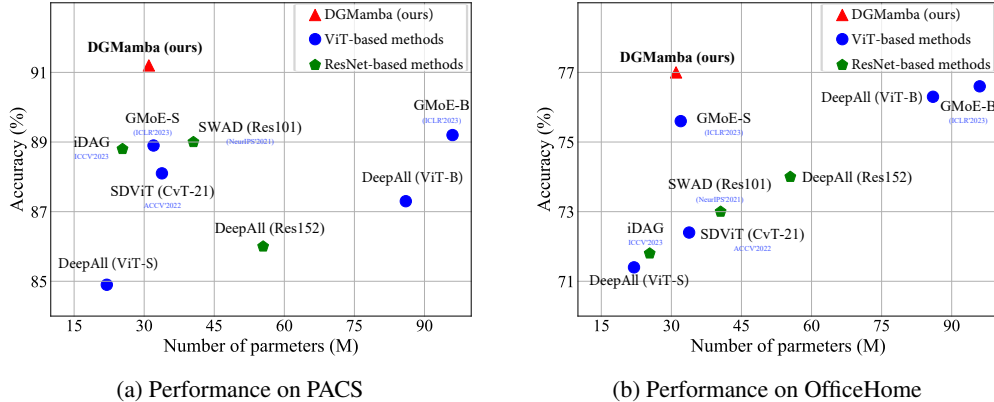


Figure 1: Comparison of current CNN-based methods, ViT-based methods, and our proposed DGMamba on PACS and OfficeHome benchmark of DG. Compared with these state-of-the-art (SOTA) methods, our proposed approach achieves the best trade-off between the generalization performance (Accuracy) and computational complexity (Number of parameters).

Recent advancements in DG [35, 50, 88] have shifted the backbone architecture from CNN [25] to ViT [11] due to its global receptive fields of self-attention layer [35, 51, 50, 22]. However, such attention layers in ViT introduce the challenge of quadratic complexity and lead to unacceptable computational inefficiency and memory overhead especially the models are very large, which makes it hard to deploy these DG methods in real-world applications.

Mamba, as an emerging state space model (SSM), possesses superior linear complexity and global receptive fields. It has been recently explored in language modeling and has a promising potential in computer vision. By employing input-dependent parameters in SSM, Mamba has exhibited promising performance in sequence data modeling and capturing long-range dependencies. In particular, VMamba [44] and Vision Mamba [101] propose to traverse the spatial domain and convert any non-causal visual image into order patch sequences. However, such SSM-based models inevitably exhibit performance degradation in unseen domains due to the lack of consideration of domain shifts and tailored designs, and there still exist generalization performance gaps compared with the state-of-the-art DG methods, *e.g.*, iDAG [30] on the PACS dataset (87.7% vs. 88.8%). Therefore, how to improve the generalizability of Mamba-based models and investigate what hinders Mamba from distribution shifts for DG is a very critical problem.

In this paper, our goal is to enhance the generalizability of Mamba-like models toward unseen domains. Our motivations mainly lie in two aspects. *Firstly*, we observe that hidden states, as an essential part of Mamba, play an important role in modeling long-range correlations by recording the historical information in sequence data, facilitating global receptive fields. However, when dealing with unseen images containing diverse domain-specific information from varying domains, such hidden states may yield undesirable effects. The domain-specific information could potentially be accumulated or even amplified in hidden states during propagation, as indicated in Figure 2 (a), thereby degrading the generalization performance. *Secondly*, how to effectively scan 2D images into 1D sequence data that is suitable for Mamba in DG is still an open problem since the pixels or patches of images do not exhibit the necessary causal relations existed in sequence data. Although recent works [101, 44, 37] have explored various scanning strategies for vision tasks, such simple 1D traverse strategies may result in unexpected domain-specific information within the generated sequence data (Figure 2(c)), thereby undermining the ability of Mamba to address distribution shifts. Besides, these fixed scanning strategies largely overlook domain-agnostic scanning and are highly sensitive to various varying scenarios, making it difficult to apply to DG.

Motivated by the above facts, we propose DGMamba, a novel State Space Model-based framework for domain generalization that excels in strong generalizability toward unseen domains and meanwhile has the advantages of global receptive fields, and efficient linear complexity. DGMamba comprises **two** key modules, Hidden State Suppressing (HSS) and Semantic-aware Patch Refining (SPR). *Firstly*, HSS is presented to eliminate the detrimental effect of non-semantic information contained in hidden states by selectively suppressing the corresponding hidden states during output prediction. By reducing non-semantic information in SSM layers, DGMamba learns domain invariant

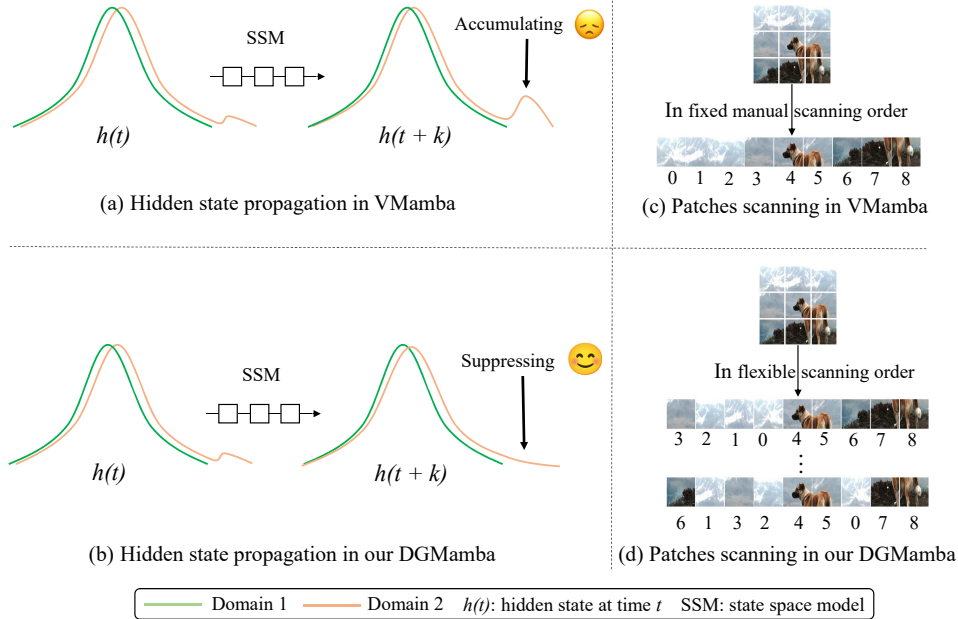


Figure 2: (a) When directly adapting VMamba to DG, domain-specific information captured by hidden states may be accumulated or even amplified during the hidden state propagation, which will impede the generalization performance. (b) In contrast, the Hidden State Suppressing (HSS) strategy is introduced in our DGMamba to alleviate the adverse effect of domain-specific information contained in hidden states. (c) Simple and fixed strategies of VMamba may result in unexpected domain-specific information within the generated sequence data when scanning 2D images into a 1D sequence, thereby undermining the ability of Mamba to address distribution shifts. (d) In contrast, the proposed Prior-Free Scanning in DGMamba endeavors to break the prior bias introduced by the fixed manual flattening, offering more meaningful sequence data.

features. *Secondly*, SPR is introduced to encourage the model to pay more attention to objects rather than context, consisting of two key designs: Prior-Free Scanning (PFS), and Domain Context Interchange (DCI). Specifically, PFS is designed to shuffle the context patches within images and contribute less to the label prediction. It provides an effective 2D scanning mechanism to traverse 2D images into 1D sequence data. As a result, PFS possesses the ability to shift the model’s attention from the context to the object. Besides, to alleviate the influence of diverse context information and local texture details across different domains, DCI replaces the context patches of images with those from different domains. The proposed DCI brings in local texture noise and regularizes the model on the combination of mismatched context and object. By leveraging both linear complexity and heterogeneous context tokens, DCI learns more robust representation efficiently. Aggregating all these contributions into one architecture, our proposed DGMamba achieves strong results on five DG benchmarks. As shown in Figure 1, compared with previous CNN-based and ViT-based methods, our DGMamba achieves the best trade-off between accuracy and parameters. In summary, we make the following contributions:

- We propose DGMamba, a novel State Space Model-based framework for domain generalization that excels in strong generalizability toward unseen domains and meanwhile has the advantages of global receptive fields and efficient linear complexity. To the best of our knowledge, this is the first work that studies the generalizability of the SSM-based model (Mamba) in domain generalization.
- We present Hidden State Suppressing (HSS) and Semantic-aware Patch Refining (SPR) to improve the generalizability of the SSM-based model. Concretely, HSS is introduced to mitigate the detrimental influence rising from the hidden states, reducing the gap between hidden states across domains. SPR, comprising two modules, namely PFS and DCI, is designed to augment the context environments to shift the model’s attention to the object.

- Extensive experiments with analyses on widely used benchmarks in DG show that our presented DGMamba achieves state-of-the-art generalization performance, showcasing its effectiveness and superiority in boosting the generalizability toward unseen domains.

## 2 Related Work

A significant amount of work has been dedicated to improving model generalization performance across diverse scenarios, including CNN-based and ViT-based methods.

**CNN-based models in DG** employ convolution neural networks, *e.g.*, Alexnet [33] and ResNet [25], to extract stronger representations. These approaches specially designed submodules to regularize the acquired features based on the CNN backbones. The most intuitive idea for DG is to minimize the empirical source risk [45, 83, 73, 1, 29]. Domain alignment [16, 39, 84, 82, 66] constrained models to convey little domain characteristics by an extra domain discriminative network. To learn domain-invariant representations, feature disentanglement methods [76, 68, 67, 40] aim to disentangle the features to acquire task-specific information. Another significant avenue is to augment the source data [58, 90, 90, 92, 64], thereby providing models with more samples with diverse styles. Inspired by the expressive performance of self-supervised learning, contrastive learning [74, 32, 47, 31, 31, 31] employed the contrastive loss function on features to reduce the gap of representation distributions in one category. Motivated by the efficacy of smooth loss landscapes in enhancing generalization performance, ensemble learning [7, 9, 32] utilized stochastic weight average to find a flatter minimum in loss spaces. Approaches based on meta-learning [85, 12, 13, 2] attempt to address the distribution shift issue during the training phase, enabling models to learn to tackle domain shifts. Despite their remarkable progress in DG and the linear complexity, the lack of global receptive fields hinders further developments of CNN-based models for boosting generalization performance [35, 44].

**ViT-based models in DG** take advantage of ViT [11] as the backbone to learn high-quality representations [75, 50], harnessing the merit of global receptive fields inherent in ViT. Discovering that the architecture of ViT aligns better with the invariant correlations than CNN [35], GMoE [35] utilized a generalizable mixture of experts to capture diverse attributes with different experts effectively. SDViT [60] attempted to tackle the overfitting in source domains by guaranteeing better prediction results from the tokens in intermediate ViT layers. TFS-ViT [50] augmented the feature stylization by token replacement. In spite of the inherent advantages in global receptive fields, ViT-based models suffer from the quadratic complexity with respect to (*w.r.t.*) the image resolution rising from the attention mechanism, leading to extra overhead of computation and memory.

**Mamba** has been widely explored in vision task [44, 80, 101, 37, 24, 71, 42, 69] to integrate both excellence of global receptive fields and linear complexity. VMamba [44] and Vim [101] proposed visual state space models to deploy Mamba for vision tasks. PCM [80] employed Mamba in point cloud analysis by introducing merged point prompts. Unfortunately, rare research has been conducted on the generalization performance of Mamba in vision tasks. To our knowledge, this is the first time that the SSM-based model Mamba has boosted the model generalization performance.

## 3 Method

In this section, we begin by introducing the concepts related to Mamba [18], *i.e.*, the State Space Model (SSM), and the selective scan mechanism. Based on this, we propose DGMamba to enhance the model generalization performance. As shown in Figure 3, DGMamba includes two core modules: Hidden State Space Suppressing (HSS), and Semantic-aware Patch Refining (SPR). HSS serves to suppress the domain-specific information conveyed in the hidden states by reducing the corresponding weighting factors. SPR encourages the model to focus more on the *object* instead of the *context*. SPR includes two core elements: Prior-Free Scanning (PFS), and Domain Context Interchange (DCI). PFS augments the range of the scanning mechanism of Mamba by randomly shuffling the non-semantic patches within images, and DCI attempts to distort images by substituting context patches with those in other domains.

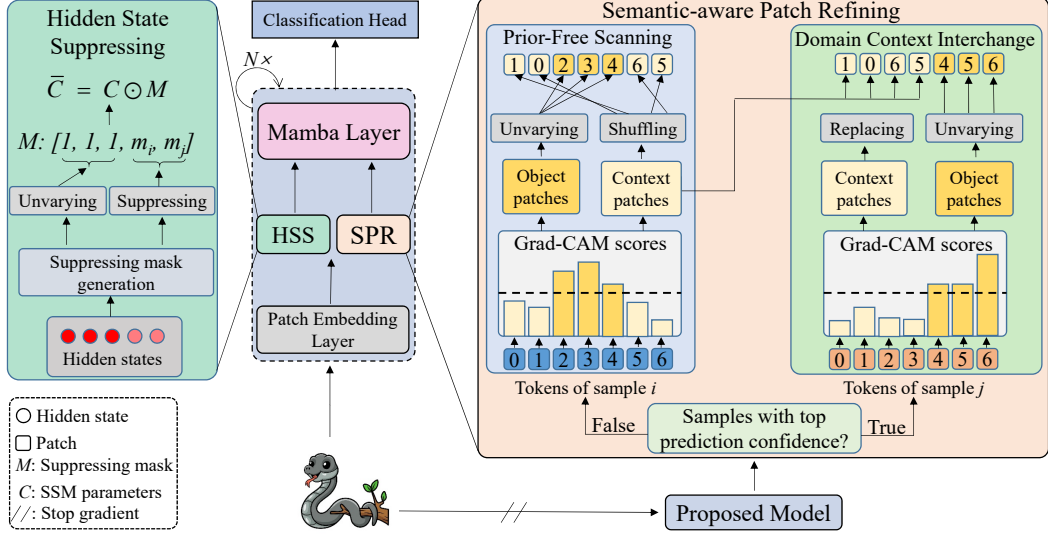


Figure 3: The framework of our proposed DGMamba. Before passing the patches into the state space layer of Mamba, the Semantic-aware Patch Refining (SPR) is employed. Concretely, for the samples not in the top percentage of prediction confidence, we apply the Prior-Free Scanning strategy to randomly shuffle the background patches that exhibit low Grad-CAM scores, providing Mamba with a more flexible and effective 2D scanning mechanism. For the remaining samples, we substitute their background patches with the context patches from diverse domains, introducing texture noise and context confusion to avoid overfitting. In addition, we employ Hidden State Suppressing (HSS) to reduce the importance of hidden states that comprise domain-specific information.

### 3.1 Preliminaries

**State Space Model (SSM).** Derived from linear time-invariant systems, SSM-based models endeavor to establish a correlation between signals  $x(t) \in \mathbb{R}^L$  and the resultant response  $y(t) \in \mathbb{R}^L$  via the hidden state  $h(t) \in \mathbb{R}^N$ . Mathematically, these models can be represented as linear ordinary differential equations (ODEs), as denoted by Eq. (1):

$$\begin{aligned} h'(t) &= Ah(t) + Bx(t), \\ y(t) &= Ch(t), \end{aligned} \quad (1)$$

where the parameters encompass  $A \in \mathbb{R}^{N \times N}$ ,  $B, C \in \mathbb{R}^N$ , with  $N$  denoting the state size.

When applied to deep learning, time-continuous SSMs require adjustment through discretization to align with the input sample rate. Based on the discretization methodology in [23], the ODE depicted in Eq. (1) can be discretized as following:

$$\begin{aligned} h_t &= \bar{A}h_{t-1} + \bar{B}x_t, \\ y_t &= Ch_t, \\ \bar{A} &= e^{\Delta A}, \\ \bar{B} &= (\Delta A)^{-1} (e^{\Delta A} - I) \cdot \Delta B, \end{aligned} \quad (2)$$

where  $\Delta$  represents the sample parameter of the inputs, facilitating the discretization process.

**2D Selective Scan Mechanism.** In addition to the challenge posed by the inconsistency between the time-continuous system and discretized signals, the characteristics of multi-media signals, such as images and videos, mismatch the architecture of the SSM-based models, which are designed to capture information within temporal signals or sequence data. As a different modal from language, images contain ample spatial information, including local texture and global shape, which may not exhibit causal correlations in sequence data. To tackle this problem, the selective scan mechanism becomes imperative. Existing methods [101, 44, 37] tend to scan images into sequence data in a fixed manner. For instance, in VMamba [44], images are flattened into two patch sequences along row

and column, respectively. VMamba models these two sequences by scanning forward and backward, respectively.

**Shortcomings of Mamba for DG.** However, the naive Mamba network encounters challenges when confronted with distribution shifts in DG, achieving a generalization performance of 87.7% on PACS dataset, inferior to the existing DG method iDAG [30] (88.8%). In the following section, we will delve into the reason behind this performance gap and propose effective strategies to assist Mamba in tackling distribution shifts for DG.

### 3.2 Hidden States Suppressing

Domain-specific information poses a great challenge for deep learning models, including the SSM-based models [44, 23, 80]. In these SSM-based models, the hidden states  $h(t)$  play an essential role in capturing long-range correlations by propagating historical information along the sequence data. It accumulates and propagates information from previous time steps, allowing the model to remember past states and information and thereby endowing the model with global receptive fields.

Despite the significant role of hidden states in Mamba, the working mechanism of hidden states could bring about negative influences when facing distribution shifts. As shown in Figure 2, when confronted with images from diverse domains, domain-specific information could also be accumulated or even be increased in hidden states, impeding model generalization performance. To mitigate the influence of accumulated domain-specific information in hidden states when predicting  $y$ , we propose to suppress the corresponding parts in the hidden states  $h(t)$ , which may carry domain-specific information.

In order to suppress the unexpected domain-specific information conveyed in the hidden states, the initial task is to recognize the hidden states that hold these adverse factors. According to the propagation rule of hidden states in Eq. (2),  $\Delta A$  (showing a positive correlation with  $\bar{A}$ ) dominates the transition of hidden states. While the hidden states  $h_t$  serve a pivotal role when predicting the output  $y_t$ . Thus, hidden states that show stronger correlations with the genuine label should be preserved more prominently during the propagation of hidden states. Consequently, they necessitate larger propagation coefficients in  $\bar{A}$ , while less associated hidden states require comparatively smaller coefficients in  $\bar{A}$ . As a result, the value of  $\Delta A$  is utilized to determine which hidden states will undergo suppression. Mathematically, the proposed Hidden States Suppressing (HSS) strategy can be formulated as follows:

$$\begin{aligned} y_t &= \bar{C}h_t, \\ \bar{C} &= C \odot M, \\ M &= (\Delta A > \alpha) + (1 - (\Delta A > \alpha)) \odot \Delta A, \end{aligned} \tag{3}$$

where  $\alpha \in [0, 0.5]$  represents the threshold for determining whether the hidden states should be suppressed. In this way, the hidden states, whose coefficient parameters  $\Delta A \leq \alpha$  will be suppressed by  $\Delta A$ , while the remaining hidden states remain the same.

### 3.3 Semantic-aware Patch Refining

In addition to the hidden state feature suppression by HSS in eliminating the adverse effect of domain-specific information, enforcing the model to pay more attention to the *object* rather than the *context* can also be an effective way to facilitate the generalization performance.

From the perspective of domain-invariant learning, *context* and *object* are two basic elements. The *object* corresponds to the foreground, which contributes most to the classification results, remaining stationary in diverse scenarios. The *context* is related to domain-specific information, such as background and image style, which varies dramatically across domains. Therefore, directing the model’s focus toward the *object* could assist in mitigating the domain-specific information. As a result, we propose Semantic-aware Patch Refining (SPR) to assist the model in better focusing on the *object*. SPR consists of two core modules: Prior-Free Scanning (PFS) and Domain Context Interchange (DCI). SPR is devoted to constructing a sufficient and random context environment, thereby breaking the adverse effect of the domain-specific information implied by the *context* in the input and enhancing generalization performance.

**Prior-Free Scanning.** Although SSM-based models [44, 101] have demonstrated excellent performance in vision tasks, a diverse and random context environment is still essential to deploy Mamba in DG. This conclusion manifests that an effective scanning mechanism is still required to tackle the challenge posed by the non-causal correlations between image pixels or patches. Suitable scanning mechanisms [44, 101, 80] should possess the ability to break unexpected spurious correlations caused by the manually created sequences of images. Nevertheless, existing SSM-based methods [44, 101, 80] are limited to scanning images into patches in a fixed unfolding approach, as indicated in Figure 2(c). These subjective traverse strategies could result in domain-specific information in the generated sequence, making it difficult for these models to address the distribution shifts in DG.

To break the spurious correlations between patches and provide an effective scanning mechanism for DG tasks, we propose Prior-Free Scanning (PFS) to address the direction-sensitive issue in Mamba. As depicted in Figure 3, PFS attempts to randomly shuffle the *context* patches, which may contribute to domain-specific information in the unfolded sequence, while keeping the *object* patches unchanged. In particular, for the representation  $z = z_c + z_o \in \mathbb{R}^{H \times W \times C}$ , where  $z_c$  and  $z_o$  represent the *context* information and *object* information, respectively, the shuffled representation  $z_{pfs}$  after the PFS strategy can be formulated as follows:

$$\begin{aligned} z_{pfs} &= z_c^s + z_o, \\ z_c^s &= Shuffle(z_c), \end{aligned} \tag{4}$$

where  $z_c^s$  denotes the shuffled *context* information by employing the  $Shuffle(\cdot)$  function in the spatial dimension. This operation could provide Mamba with sequence data exhibiting flexible scanning direction by generating *context* disturbance or noise while keeping the consistent *object* information. As a result, it mitigates the domain-specific information brought by the manual fixed flattening strategy and breaks the spurious correlations.

**Domain Context Interchange.** The proposed PFS facilitates the model to pay more attention to the *object* instead of the *context* within images. However, the *context* information is heterogeneous across varying domains in DG. The *context* patch shuffling in PFS is limited in the given scenarios, inadequate to provide sufficient diverse *context* information for removing the domain-specific information. Besides, the heterogeneous *context* patches from different domains not only exhibit diverse *context* information but also encompass distinct local texture characteristics.

To sufficiently tackle the adverse influence of heterogeneous *context* and diverse local texture details, we propose to create ample *context* scenarios and introduce local texture noise by Domain Context Interchange (DCI). As shown in the Domain Context Interchange module in Figure 3, DCI substitutes the image *context* patches with those from different domains. This operation regularizes the model on the counterfactual samples [72, 8], *i.e.*, the combination of semantic information in one domain and non-semantic features from different domains. This strategy further forces models to focus on the generalizable features while discarding the textual details or other domain-specific features.

In implementation, DCI only performs on samples with high confidence in the classification results, while other samples remain unchanged. As the samples exhibiting high classification confidence may result in overfitting in their scenarios, replacing their *context* patches with those from different domains could introduce challenging *context* noise to generate heterogeneous *context* and local texture noise. While remaining samples may struggle to recognize the *object* from the *context*, conducting DCI on them could further increase the difficulty in learning generalizable presentations. Specifically, we only apply DCI to the top 20% of batch samples according to the classification confidence based on the negative cross-entropy loss. These samples with high negative cross-entropy loss are easy samples for the model, leading to inflated confidence in their classification, which may, in turn, result in overfitting problems.

**Context Patch identifying.** To distinguish the *context* and *object* patches, we take advantage of Grad-CAM [57] as the metric to measure the contributions of different regions of images. As the regions containing the *object* would activate the Grad-CAM greatly, while the patches exhibiting the *context* possess a low value in the Grad-CAM, we split the image patches into *context* and *object* according to their values in the activation map generated by Grad-CAM. Specifically, the patches with the smallest 25% Grad-CAM values are determined as the *context* information  $z_c$ , while the remaining are used as *object* information  $z_o$ .

Table 1: Results on PACS with our DGMamba. The best results are bolded.

Method	Backbone	Venue	Target domain				Avg.(↑)
			Art	Cartoon	Photo	Sketch	
GroupDRO [55]	ResNet50	ICLR’2019	83.5	79.1	96.7	78.3	84.4
VREx [34]	ResNet50	ICML’2021	86.0	79.1	96.9	77.7	84.9
RSC [29]	ResNet50	ECCV’2020	85.4	79.7	97.6	78.2	85.2
MTL [6]	ResNet50	JMLR’2021	87.5	77.1	96.4	77.3	84.6
Mixstyle [91]	ResNet50	ICLR’2021	86.8	79.0	96.6	78.5	85.2
SagNet [49]	ResNet50	CVPR’2021	87.4	80.7	97.1	80.0	86.3
ARM [79]	ResNet50	NeurIPS’2021	86.8	76.8	97.4	79.3	85.1
SWAD [7]	ResNet50	NeurIPS’2021	89.3	83.4	97.3	82.5	88.1
PCL [74]	ResNet50	CVPR’2022	90.2	83.9	98.1	82.6	88.7
SAGM [65]	ResNet50	CVPR’2023	87.4	80.2	98.0	80.8	86.6
iDAG [30]	ResNet50	ICCV’2023	90.8	83.7	98.0	82.7	88.8
GMDG [61]	ResNet50	CVPR’2024	84.7	81.7	97.5	80.5	85.6
SDViT [60]	DeiT-S	ACCV’2022	87.6	82.4	98.0	77.2	86.3
GMoE [35]	DeiT-S	ICLR’2023	89.4	83.9	<b>99.1</b>	74.5	86.7
DGMamba	VMamba-T	-	<b>91.3</b>	<b>87.0</b>	99.0	<b>87.3</b>	<b>91.2</b>

Table 2: Results on VLCS with our DGMamba. The best results are bolded.

Method	Backbone	Venue	Target domain				Avg.(↑)
			Caltech	LabelMe	SUN	PASCAL	
GroupDRO [55]	ResNet50	ICLR’2019	97.3	63.4	69.5	76.7	76.7
VREx [34]	ResNet50	ICML’2021	98.4	64.4	74.1	76.2	78.3
RSC [29]	ResNet50	ECCV’2020	97.9	62.5	72.3	75.6	77.1
MTL [6]	ResNet50	JMLR’2021	97.8	64.3	71.5	75.3	77.2
Mixstyle [91]	ResNet50	ICLR’2021	98.6	64.5	72.6	75.7	77.9
SagNet [49]	ResNet50	CVPR’2021	97.9	64.5	71.4	77.5	77.8
ARM [79]	ResNet50	NeurIPS’2021	98.7	63.6	71.3	76.7	77.6
SWAD [7]	ResNet50	NeurIPS’2021	98.8	63.3	75.3	79.2	79.1
PCL [74]	ResNet50	CVPR’2022	99.0	63.6	73.8	75.6	78.0
SAGM [65]	ResNet50	CVPR’2023	<b>99.0</b>	65.2	75.1	80.7	80.0
iDAG [30]	ResNet50	ICCV’2023	98.1	62.7	69.9	77.1	76.9
GMDG [61]	ResNet50	CVPR’2024	98.3	<b>65.9</b>	73.4	79.3	79.2
SDViT [60]	DeiT-S	ACCV’2022	96.8	64.2	76.2	78.5	78.9
GMoE [35]	DeiT-S	ICLR’2023	96.9	63.2	72.3	79.5	78.0
DGMamba	VMamba-T	-	98.9	64.3	<b>79.2</b>	<b>80.8</b>	<b>80.8</b>

## 4 Experiments

**Dataset.** Following standard protocol in DG [20, 7], we evaluate the effectiveness of our proposed DGMamba and compare it with state-of-the-art methods in DG on five commonly used benchmarks: (1) PACS [36] includes 9991 images categorized into 7 classes exhibiting 4 styles. (2) VLCS [14] involves four datasets, totaling 10729 images distributed in 5 categories. (3) OfficeHome [63] comprises 15588 images in 65 classes from 4 datasets. (4) TerraIncognita [4] encompasses 24330 photographs of 10 kinds of animals taken at 4 diverse locations. (5) DomainNet [52] comprises 586575 images categorized into 345 classes from six domains.

**Implementation details.** Our proposed model employs Mamba [18] as the backbone, which is pretrained on ImageNet [10]. Following VMamba [44], the network comprises 4 blocks, each



Table 3: Results on OfficeHome with our DGMamba. The best results are bolded.

Method	Backbone	Venue	Target domain				Avg.(↑)
			Art	Clipart	Product	Real	
GroupDRO [55]	ResNet50	ICLR'2019	60.4	52.7	75.0	76.0	66.0
VREx [34]	ResNet50	ICML'2021	60.7	53.0	75.3	76.6	66.4
RSC [29]	ResNet50	ECCV'2020	60.7	51.4	74.8	75.1	65.5
MTL [6]	ResNet50	JMLR'2021	61.5	52.4	74.9	76.8	66.4
Mixstyle [91]	ResNet50	ICLR'2021	51.1	53.2	68.2	69.2	60.4
SagNet [49]	ResNet50	CVPR'2021	63.4	54.8	75.8	78.3	68.1
ARM [79]	ResNet50	NeurIPS'2021	58.9	51.0	74.1	75.2	64.8
SWAD [7]	ResNet50	NeurIPS'2021	66.1	57.7	78.4	80.2	70.6
PCL [74]	ResNet50	CVPR'2022	67.3	59.9	78.7	80.7	71.6
SAGM [65]	ResNet50	CVPR'2023	65.4	57.0	78.0	80.0	70.1
iDAG [30]	ResNet50	ICCV'2023	68.2	57.9	79.7	81.4	71.8
GMDG [61]	ResNet50	CVPR'2024	68.9	56.2	79.9	82.0	70.7
SDViT [60]	DeiT-S	ACCV'2022	68.3	56.3	79.5	81.8	71.5
GMoE [35]	DeiT-S	ICLR'2023	69.3	58.0	79.8	82.6	72.4
DGMamba	VMamba-T	-	<b>76.2</b>	<b>61.8</b>	<b>83.9</b>	<b>86.1</b>	<b>77.0</b>

Table 4: Results on TerraIncognita with our DGMamba. The best results are bolded.

Method	Backbone	Venue	Target domain				Avg.(↑)
			L100	L38	L43	L46	
GroupDRO [55]	ResNet50	ICLR'2019	41.2	38.6	56.7	36.4	43.2
VREx [34]	ResNet50	ICML'2021	48.2	41.7	56.8	38.7	46.4
RSC [29]	ResNet50	ECCV'2020	50.2	39.2	56.3	40.8	46.6
MTL [6]	ResNet50	JMLR'2021	49.3	39.6	55.6	37.8	45.6
Mixstyle [91]	ResNet50	ICLR'2021	54.3	34.1	55.9	31.7	44.0
SagNet [49]	ResNet50	CVPR'2021	53.0	43.0	57.9	40.4	48.6
ARM [79]	ResNet50	NeurIPS'2021	49.3	38.3	55.8	38.7	45.5
SWAD [7]	ResNet50	NeurIPS'2021	55.4	44.9	59.7	39.9	50.0
PCL [74]	ResNet50	CVPR'2022	58.7	46.3	60.0	43.6	52.1
SAGM [65]	ResNet50	CVPR'2023	54.8	41.4	57.7	41.3	48.8
iDAG [30]	ResNet50	ICCV'2023	58.7	35.1	57.5	33.0	46.1
GMDG [61]	ResNet50	CVPR'2024	59.8	45.3	57.1	38.2	50.1
SDViT [60]	DeiT-S	ACCV'2022	55.9	31.7	52.2	37.4	44.3
GMoE [35]	DeiT-S	ICLR'2023	59.2	34.0	50.7	38.5	45.6
DGMamba	VMamba-T	-	<b>62.7</b>	<b>48.3</b>	<b>61.1</b>	<b>46.4</b>	<b>54.6</b>

consisting of 2, 2, 4, and 2 Mamba layers, respectively. Down-sampling is incorporated before each block. Additionally, bidirectional Mamba is utilized to enable each patch to gather information from any other patches. Following the training configuration in existing DG approaches [20, 7, 35], the model undergoes training for 10000 iterations, with a batch size of 16 for each source domain. For optimization, we employ the AdamW optimizer with betas of (0.9, 0.999) and a momentum of 0.9. We incorporate a cosine decay learning rate scheduler. The initial learning rate is searched in [3e-4, 4.5e-4].

#### 4.1 Main results

**Results on PACS dataset.** Table 1 reports the generalization performance on PACS, indicating the best generalization performance of our proposed DGMamba across almost all these domains.

Table 5: Results on DomainNet with our DGMamba. The best results are bolded.

Method	Backbone	Venue	Target domain						Avg.(↑)
			Clipart	Infograph	painting	Quickdraw	Real	Sketch	
GroupDRO [55]	ResNet50	ICLR'2019	47.2	17.5	33.8	9.3	51.6	40.1	33.3
VREx [34]	ResNet50	ICML'2021	47.3	16.0	35.8	10.9	49.6	42.0	33.6
RSC [29]	ResNet50	ECCV'2020	55.0	18.3	44.4	12.2	55.7	47.8	38.9
MTL [6]	ResNet50	JMLR'2021	57.9	18.5	46.0	12.5	59.5	49.2	40.6
Mixstyle [91]	ResNet50	ICLR'2021	51.9	13.3	37.0	12.3	46.1	43.4	34.0
SagNet [49]	ResNet50	CVPR'2021	57.7	19.0	45.3	12.7	58.1	48.8	40.3
ARM [79]	ResNet50	NeurIPS'2021	49.7	16.3	40.9	9.4	53.4	43.5	35.5
SWAD [7]	ResNet50	NeurIPS'2021	66.0	22.4	53.5	16.1	65.8	55.5	46.5
PCL [74]	ResNet50	CVPR'2022	67.9	24.3	55.3	15.7	66.6	56.4	47.7
SAGM [65]	ResNet50	CVPR'2023	64.9	21.1	51.5	14.8	64.1	53.6	45.0
iDAG [30]	ResNet50	ICCV'2023	67.9	24.2	55.0	16.4	66.1	56.9	47.7
GMDG [61]	ResNet50	CVPR'2024	63.4	22.4	51.4	13.4	64.4	52.4	44.6
SDViT [60]	DeiT-S	ACCV'2022	63.4	22.9	53.7	15.0	67.4	52.6	45.8
GMoE [35]	DeiT-S	ICLR'2023	<b>68.2</b>	24.7	55.7	16.3	69.1	55.4	48.3
DGMamba	VMamba-T	-	67.0	<b>27.9</b>	<b>56.5</b>	<b>18.4</b>	<b>69.5</b>	<b>57.9</b>	<b>49.6</b>

Notably, DGMamba surpasses the SOTA methods by 2.7% in average generalization performance. Besides, on the hard-to-transfer domains, such as ‘Cartoon’ and ‘Sketch,’ our approach beats the second-best method approaches by 3.9% and 5.6%, respectively, demonstrating the effectiveness of our DGMamba in enhancing generalization capacity.

**Results on VLCS dataset.** As shown in Table 2, the proposed DGMamba demonstrates superior average generalization performance compared to SOTA methods. In addition, our method consistently ranks among the top three performers in three out of the four environments, indicating its efficacy in improving the model generalization performance.

**Results on OfficeHome dataset.** The generalization results on OfficeHome are shown in Table 3. The proposed DGMamba has achieved a significant enhancement in generalization performance in all scenarios. Remarkably, DGMamba outperforms the SOTA method by 6.4% in average generalization performance. These findings showcase the superiority of DGMamba in acquiring robust representations.

**Results on TerraIncognita datasets.** We provide the experiment results on TerraIncognita in Table 4. Our proposed DGMamba attains the best generalization performance across all environments. Notably, our proposed approach achieves a 4.8% gain over the SOTA method in average generalization performance. These outcomes highlight DGMamba’s outstanding ability to obtain domain-invariant representations.

**Results on DomainNet datasets.** To further assess the efficacy of mitigating distribution shifts in large-scale benchmarks, we test the proposed DGMamba on DomainNet [52] and compare it with state-of-the-art DG methods. As illustrated by Table 5, our proposed DGMamba demonstrates a substantial improvement of 2.7% compared to the state-of-the-art approach in terms of average generalization performance across diverse domains. Remarkably, our DGMamba attains the best performance in five out of the six domains. These findings underscore the superiority of the proposed DGMamba in tackling distribution shifts in real-world applications.

## 4.2 Ablation study and analysis

**Effectiveness of each component.** We conduct an ablation study on PACS to disclose the contributions of our proposed modules on the generalization performance. As indicated in Table 6, the proposed HSS, PFS, and DCI consistently facilitate the enhancement of the generalization performance across almost all scenarios, demonstrating their effectiveness in capturing genuine correlations and removing domain-specific information. Specifically, in the hardest-to-transfer domain where the DeepAll behaves poorly, *i.e.*, ‘Sketch’, HSS shows the greatest enhancement, with an increase of 2.6%. This underscores the superiority of HSS in mitigating the domain-specific information carried in hidden states. The proposed PFS could also enhance the performance in the remaining domains,

Table 6: Ablation study on PACS with our proposed key modules.

Method	Target domain				Avg.(↑)
	Art	Cartoon	Photo	Sketch	
VMamba [44]	88.2	86.2	98.4	84.9	89.4
w/ HSS	90.4	86.8	98.8	87.1	90.8
w/ PFS	91.8	85.9	98.7	85.4	90.5
w/ DCI	<b>91.8</b>	85.8	99.0	85.3	90.4
DGMamba	91.3	<b>87.0</b>	<b>99.0</b>	<b>87.3</b>	<b>91.2</b>

Figure 4: Effect of  $\alpha$  in the proposed Hidden State Suppressing on PACS.

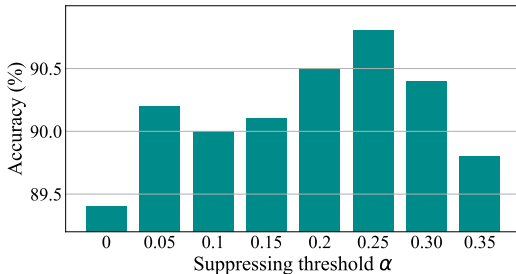


Table 7: Effectiveness of our proposed SPR when inserting at different state space blocks of DGMamba on PACS.

Block	Target domain				Avg.(↑)
	Art	Cartoon	Photo	Sketch	
None	88.2	86.2	98.4	84.9	89.4
Block 3	91.7	<b>86.8</b>	98.9	82.7	90.0
Block 2	91.7	86.5	98.9	83.9	90.2
Block 1	<b>92.3</b>	86.3	<b>99.1</b>	<b>85.4</b>	<b>90.8</b>

Table 8: Comparison of the proposed Hidden State Suppressing (HSS) with Hidden State Masking (HSM) on PACS using recognition accuracy (%).

Threshold	0	0.15	0.2	0.25
HSM	89.4	90.2	90.3	90.1
HSS	89.4	90.1	90.5	90.8

underscoring that offering a more effective scanning strategy and directing the model’s focus on the object are beneficial to improving generalization capacity. In addition, the heterogeneous context and texture noise introduced by DCI can also promote the model to shift attention to domain invariant features. Moreover, the combination of these proposed modules reaches the highest performance, indicating the necessity of these modules in yielding optimal performance enhancement.

**SPR at different layers.** We insert the SPR module at different layers of VMamba and showcase diverse performance gains in Table 7. The shallow layers contain more spurious correlations, and thereby, should benefit more from the proposed SPR module than the deeper layers, which hold more correlations with the prediction results. This inference is also supported by the generalization performance in Table 7. The highest gains in generalization performance have been achieved when inserting the SPR module before Block 1.

**Effect of  $\alpha$  in HSS.** The threshold  $\alpha$  in HSS controls the number of hidden states to be suppressed. Intuitively, more suppressed hidden states would eliminate more domain-specific information, thereby enhancing generalization performance. Figure 4 reports the generalization performance of our HSS by varying  $\alpha$ , indicating that the best performance can be obtained by HSS when the threshold  $\alpha$  is set to 0.25. This observation demonstrates the effectiveness of HSS in mitigating the detrimental effect of domain-specific features on generalization. However, it is noteworthy that a relatively large  $\alpha$  would also mitigate the positive influences of hidden states associated with the valuable features for predictions, consequently degrading the generalization performance.

**Hidden State Suppressing (HSS) v.s. Hidden State Masking (HSM).** In practice, we also experiment with a hidden state masking strategy to eliminate the adverse effect of domain-specific information. HSM just attempts to discard the hidden states associated with domain-specific information, assuming these hidden states contribute little to the prediction results. However, as indicated in Table 8, although exhibiting the ability to enhance generalization performance, HSM is less competitive than the proposed HSS. The result demonstrates that these hidden states deserve to be suppressed and may also convey essential semantic information to capture long-range correlations.

**Computation Efficiency.** To assess the computational efficiency of our proposed DGMamba, we conduct experiments on PACS to compare it with SOTA methods from different perspectives, including model parameters, float-point-operations per second (Flops), inference time and their generalization performance on PACS. It is worth noting that iDAG [30] requires multiple samples in the training phase, thus we create a tensor with batch size 2 to evaluate its GFlops. For the remaining

Table 9: Comparison of the computational efficiency of existing SOTA methods in DG and our DGMamba on PACS. Tested with an image size of  $224 \times 224$  on one NVIDIA Tesla V100 GPU.

Model	Backbone	Params (M)	GFlops (G)	Time (ms)	Acc (%)
iDAG [30] (ICCV’2023)	ResNet50	25	8	94	88.8
iDAG [30] (ICCV’2023)	ResNet101	43	15	495	89.2
GMoE-S [35] (ICLR’2023)	DeiT-S	34	5	136	88.1
GMoE-B [35] (ICLR’2023)	DeiT-B	133	19	361	89.2
VMamba [44] (Arxiv’2024)	VMamba-T	31	5	225	89.4
DGMamba (ours)	VMamba-T	31	5	233	91.2

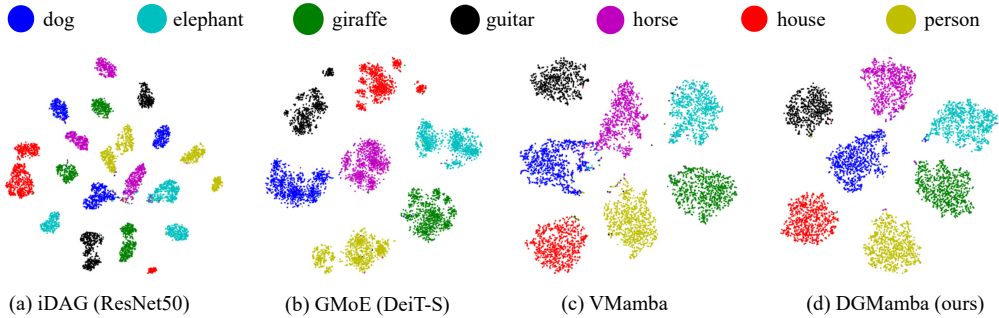


Figure 5: Visualizations with t-SNE embeddings [62] illustrating various classes’ representations produced by (a) iDAG [30], (b) GMoE [35], (c) VMamba [44], and (d) DGMamba (ours), respectively. DGMamba demonstrates the superior clustering effect. Zoom in for details.

methods, the dimension of batch size for evaluating Flops is set to 1. The inference time is averaged over 100 experiments. As indicated in Table 9, while our proposed DGMamba exhibits relatively fewer parameters and GFlops than existing SOTA methods based on CNN or ViT, it still achieves the highest generalization performance.

**Feature Visualization.** To visually demonstrate the impact of our proposed DGMamba, we adopt t-SNE embeddings [62] to investigate the feature characteristics. Concretely, we conduct experiments on PACS with ‘Photo’ as the target domain. Figure 5 depicts the feature visualizations based on the CNN-based method iDAG [30], ViT-based method GMoE [35], VMamba [44], and our proposed DGMamba, respectively. Remarkably, DGMamba acquires superior representations, exhibiting enhanced intra-class compactness and inter-class discrimination, especially in comparison with iDAG and GMoE. Besides, the enhancement of DGMamba relative to VMamba is also obvious. Firstly, the distinction between features of ‘dog’ (blue) and ‘horse’ (purple) in DGMamba is more pronounced. Secondly, the features within the same category in DGMamba manifest increased compactness. These findings confirm the superiority of DGMamba in boosting model generalization capacity.

**Activation Map Visualization.** To further visually verify the outstanding prediction mechanism of our proposed DGMamba, we provide visualizations for the activation maps of the last state space layer with Grad-CAM [57]. The results are reported in Figure 6, demonstrating that our proposed DGMamba can still capture the semantically related information, *i.e.*, the global shape and the object itself, when confronted with hard samples exhibiting significant disparity from the real world. Taking the ‘dog’ for instance, our proposed DGMamba is able to focus on the entire dog face, while the baseline VMamba suffers from recognizing these critical features. In addition, VMamba can be easily interfered by the background and the texture details, exemplified by the ‘house’ and ‘person’. While our DGMamba can still comprehensively learn the object information even with such complex domain-specific information. These findings highlight the excellence of our method in improving model generalization capacity.

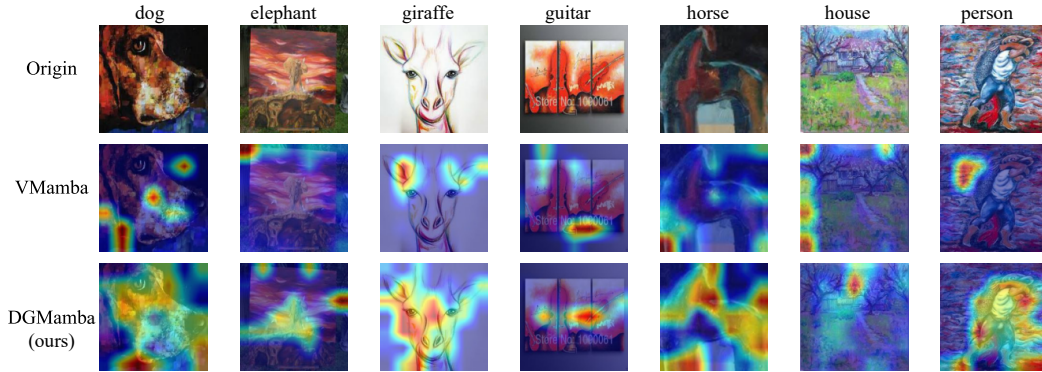


Figure 6: Visualization for the activation maps of the last state space layer on PACS with “Art” as the target domain. For each sample, the first row represents the original image, the middle row is the activation map generated by VMamba without any domain generalization techniques, and the last row denotes the activation map captured by our proposed DGMamba.

## 5 Conclusion

This work is the first endeavor to explore the generalizability of the SSM-based model (Mamba) in DG. We propose a novel framework named DGMamba, that contains two pivotal techniques. Firstly, we design a novel Hidden State Suppressing to alleviate the adverse effect of domain-specific information conveyed in hidden states. Secondly, we propose Semantic-aware Patch Refining, which consists of Prior-Free Scanning and Domain Context Interchange. Both aim to direct the model’s focus toward the object rather than the context. Extensive experiments on five widely used DG benchmarks show the superiority of DGMamba compared with SOTA DG methods based on CNN or ViT. We believe our work builds a solid baseline for exploiting SSMs for the DG community.

**Future work.** In the future, we would like to investigate the feature prompt or domain prompt to facilitate SSM-based models learning more powerful representations for DG. This strategy has demonstrated effectiveness in guiding model learning with ViT. Besides, it is valuable to delve further into Mamba architecture in high-structure tasks to unleash its potential in addressing distribution shifts, such as domain-generalized semantic segmentation and domain-generalized object detection.

## References

- [1] Martin Arjovsky, Léon Bottou, Ishaan Gulrajani, and David Lopez-Paz. Invariant risk minimization. *arXiv preprint arXiv:1907.02893*, 2019. 4
- [2] Yogesh Balaji, Swami Sankaranarayanan, and Rama Chellappa. Metareg: Towards domain generalization using meta-regularization. *Advances in neural information processing systems*, 31, 2018. 4
- [3] Andrei Barbu, David Mayo, Julian Alverio, William Luo, Christopher Wang, Dan Gutfreund, Josh Tenenbaum, and Boris Katz. Objectnet: A large-scale bias-controlled dataset for pushing the limits of object recognition models. *Advances in neural information processing systems*, 32, 2019. 1
- [4] Sara Beery, Grant Van Horn, and Pietro Perona. Recognition in Terra Incognita. In *Proceedings of the European Conference on Computer Vision (ECCV)*, pages 456–473, 2018. 1, 8, 19
- [5] Shai Ben-David, John Blitzer, Koby Crammer, Alex Kulesza, Fernando Pereira, and Jennifer Wortman Vaughan. A theory of learning from different domains. *Machine learning*, 79(1):151–175, 2010. 1
- [6] Gilles Blanchard, Aniket Anand Deshmukh, Ürun Dogan, Gyemin Lee, and Clayton Scott. Domain generalization by marginal transfer learning. *The Journal of Machine Learning Research*, 22(1):46–100, 2021. 8, 9, 10, 20
- [7] Junbum Cha, Sanghyuk Chun, Kyungjae Lee, Han-Cheol Cho, Seunghyun Park, Yunsung Lee, and Sungrae Park. Swad: Domain generalization by seeking flat minima. *Advances in Neural Information Processing Systems*, 34:22405–22418, 2021. 4, 8, 9, 10, 19, 20
- [8] Chaoqi Chen, Luyao Tang, Feng Liu, Gangming Zhao, Yue Huang, and Yizhou Yu. Mix and reason: Reasoning over semantic topology with data mixing for domain generalization. *Advances in Neural Information Processing Systems*, 35:33302–33315, 2022. 1, 7
- [9] Xu Chu, Yujie Jin, Wenwu Zhu, Yasha Wang, Xin Wang, Shanghang Zhang, and Hong Mei. DNA: Domain Generalization with Diversified Neural Averaging. In *Proceedings of the 39th International Conference on Machine Learning*, pages 4010–4034. PMLR, 2022. 4
- [10] Jia Deng, Wei Dong, Richard Socher, Li-Jia Li, Kai Li, and Li Fei-Fei. Imagenet: A large-scale hierarchical image database. In *2009 IEEE conference on computer vision and pattern recognition*, pages 248–255. Ieee, 2009. 8
- [11] Alexey Dosovitskiy, Lucas Beyer, Alexander Kolesnikov, Dirk Weissenborn, Xiaohua Zhai, Thomas Unterthiner, Mostafa Dehghani, Matthias Minderer, Georg Heigold, Sylvain Gelly, Jakob Uszkoreit, and Neil Houlsby. An Image is Worth 16x16 Words: Transformers for Image Recognition at Scale. In *International Conference on Learning Representations*, 2020. 2, 4
- [12] Qi Dou, Daniel Coelho de Castro, Konstantinos Kamnitsas, and Ben Glocker. Domain generalization via model-agnostic learning of semantic features. *Advances in neural information processing systems*, 32, 2019. 4
- [13] Yingjun Du, Jun Xu, Huan Xiong, Qiang Qiu, Xiantong Zhen, Cees GM Snoek, and Ling Shao. Learning to learn with variational information bottleneck for domain generalization. In *European conference on computer vision*, pages 200–216. Springer, 2020. 4
- [14] Chen Fang, Ye Xu, and Daniel N Rockmore. Unbiased metric learning: On the utilization of multiple datasets and web images for softening bias. In *Proceedings of the IEEE International Conference on Computer Vision*, pages 1657–1664, 2013. 8, 19
- [15] Tongtong Fang, Nan Lu, Gang Niu, and Masashi Sugiyama. Rethinking importance weighting for deep learning under distribution shift. *Advances in Neural Information Processing Systems*, 33:11996–12007, 2020. 1
- [16] Yaroslav Ganin, Evgeniya Ustinova, Hana Ajakan, Pascal Germain, Hugo Larochelle, François Laviolette, Mario March, and Victor Lempitsky. Domain-Adversarial Training of Neural Networks. *Journal of Machine Learning Research*, 17(59):1–35, 2016. 1, 4
- [17] Robert Geirhos, Kantharaju Narayanappa, Benjamin Mitzkus, Tizian Thieringer, Matthias Bethge, Felix A Wichmann, and Wieland Brendel. Partial success in closing the gap between human and machine vision. *Advances in Neural Information Processing Systems*, 34:23885–23899, 2021. 1
- [18] Albert Gu and Tri Dao. Mamba: Linear-time sequence modeling with selective state spaces. *arXiv preprint arXiv:2312.00752*, 2023. 4, 8
- [19] Qiqi Gu, Qianyu Zhou, Minghao Xu, Zhengyang Feng, Guangliang Cheng, Xuequan Lu, Jianping Shi, and Lizhuang Ma. Pit: Position-invariant transform for cross-fov domain adaptation. In *Proceedings of the IEEE/CVF International Conference on Computer Vision*, pages 8761–8770, 2021. 1
- [20] Ishaan Gulrajani and David Lopez-Paz. In search of lost domain generalization. In *International Conference on Learning Representations*, 2020. 1, 8, 9, 19
- [21] Jintao Guo, Lei Qi, and Yinghuan Shi. Domaindrop: Suppressing domain-sensitive channels for domain generalization. In *Proceedings of the IEEE/CVF International Conference on Computer Vision*, pages 19114–19124, 2023. 1
- [22] Jintao Guo, Lei Qi, Yinghuan Shi, and Yang Gao. Seta: Semantic-aware token augmentation for domain generalization. *arXiv preprint arXiv:2403.11792*, 2024. 2

- [23] Ankit Gupta, Albert Gu, and Jonathan Berant. Diagonal state spaces are as effective as structured state spaces. *Advances in Neural Information Processing Systems*, 35:22982–22994, 2022. 5, 6
- [24] Haoyang He, Yuhu Bai, Jiangning Zhang, Qingdong He, Hongxu Chen, Zhenye Gan, Chengjie Wang, Xiangtai Li, Guanzhong Tian, and Lei Xie. Mambaad: Exploring state space models for multi-class unsupervised anomaly detection. *arXiv*, 2024. 4
- [25] Kaiming He, Xiangyu Zhang, Shaoqing Ren, and Jian Sun. Deep Residual Learning for Image Recognition. In *Proceedings of the IEEE Conference on Computer Vision and Pattern Recognition*, pages 770–778, 2016. 2, 4
- [26] Lu He, Qianyu Zhou, Xiangtai Li, Li Niu, Guangliang Cheng, Xiao Li, Wenxuan Liu, Yunhai Tong, Lizhuang Ma, and Liqing Zhang. End-to-end video object detection with spatial-temporal transformers. In *Proceedings of the 29th ACM International Conference on Multimedia*, pages 1507–1516, 2021. 1
- [27] Dan Hendrycks, Steven Basart, Norman Mu, Saurav Kadavath, Frank Wang, Evan Dorundo, Rahul Desai, Tyler Zhu, Samyak Parajuli, Mike Guo, et al. The many faces of robustness: A critical analysis of out-of-distribution generalization. In *Proceedings of the IEEE/CVF international conference on computer vision*, pages 8340–8349, 2021. 1
- [28] Dan Hendrycks, Kevin Zhao, Steven Basart, Jacob Steinhardt, and Dawn Song. Natural adversarial examples. In *Proceedings of the IEEE/CVF conference on computer vision and pattern recognition*, pages 15262–15271, 2021. 1
- [29] Zeyi Huang, Haohan Wang, Eric P Xing, and Dong Huang. Self-challenging improves cross-domain generalization. In *European Conference on Computer Vision*, pages 124–140. Springer, 2020. 4, 8, 9, 10, 20
- [30] Zenan Huang, Haobo Wang, Junbo Zhao, and Nenggan Zheng. idag: Invariant dag searching for domain generalization. In *Proceedings of the IEEE/CVF International Conference on Computer Vision*, pages 19169–19179, 2023. 1, 2, 6, 8, 9, 10, 11, 12, 20, 21
- [31] Seogkyu Jeon, Kibeom Hong, Pilhyeon Lee, Jewook Lee, and Hyeran Byun. Feature stylization and domain-aware contrastive learning for domain generalization. In *Proceedings of the 29th ACM International Conference on Multimedia*, pages 22–31, 2021. 4
- [32] Daehee Kim, Youngjun Yoo, Seunghyun Park, Jinkyu Kim, and Jaekoo Lee. Selfreg: Self-supervised contrastive regularization for domain generalization. In *Proceedings of the IEEE/CVF International Conference on Computer Vision*, pages 9619–9628, 2021. 1, 4
- [33] Alex Krizhevsky, Ilya Sutskever, and Geoffrey E Hinton. ImageNet Classification with Deep Convolutional Neural Networks. In *Advances in Neural Information Processing Systems*, volume 25. Curran Associates, Inc., 2012. 4
- [34] David Krueger, Ethan Caballero, Joern-Henrik Jacobsen, Amy Zhang, Jonathan Binas, Dinghui Zhang, Remi Le Priol, and Aaron Courville. Out-of-distribution generalization via risk extrapolation (rex). In *International Conference on Machine Learning*, pages 5815–5826. PMLR, 2021. 8, 9, 10, 20
- [35] Bo Li, Yifei Shen, Jingkan Yang, Yezhen Wang, Jiawei Ren, Tong Che, Jun Zhang, and Ziwei Liu. Sparse mixture-of-experts are domain generalizable learners. In *The Eleventh International Conference on Learning Representations*, 2023. 2, 4, 8, 9, 10, 12, 19, 20, 21
- [36] Da Li, Yongxin Yang, Yi-Zhe Song, and Timothy M. Hospedales. Deeper, Broader and Artier Domain Generalization. In *2017 IEEE International Conference on Computer Vision (ICCV)*, pages 5543–5551, 2017. 8, 19
- [37] Kunchang Li, Xinhao Li, Yi Wang, Yanan He, Yali Wang, Limin Wang, and Yu Qiao. Videomamba: State space model for efficient video understanding, 2024. 2, 4, 5
- [38] Xiangtai Li, Haobo Yuan, Wei Li, Henghui Ding, Size Wu, Wenwei Zhang, Yining Li, Kai Chen, and Chen Change Loy. Omg-seg: Is one model good enough for all segmentation? In *CVPR*, 2024. 1
- [39] Ya Li, Xinmei Tian, Mingming Gong, Yajing Liu, Tongliang Liu, Kun Zhang, and Dacheng Tao. Deep Domain Generalization via Conditional Invariant Adversarial Networks. In *Proceedings of the European Conference on Computer Vision (ECCV)*, pages 624–639, 2018. 4
- [40] Chang Liu, Lichen Wang, Kai Li, and Yun Fu. Domain generalization via feature variation decorrelation. In *Proceedings of the 29th ACM International Conference on Multimedia*, pages 1683–1691, 2021. 4
- [41] Fengqi Liu, Jingyu Gong, Qianyu Zhou, Xuequan Lu, Ran Yi, Yuan Xie, and Lizhuang Ma. Cloudmix: Dual mixup consistency for unpaired point cloud completion. *IEEE Transactions on Visualization and Computer Graphics*, 2024. 1
- [42] Jiarun Liu, Hao Yang, Hong-Yu Zhou, Yan Xi, Lequan Yu, Yizhou Yu, Yong Liang, Guangming Shi, Shaoting Zhang, Hairong Zheng, et al. Swin-umamba: Mamba-based unet with imagenet-based pretraining. *arXiv preprint arXiv:2402.03302*, 2024. 4
- [43] Ye Liu, Lingfeng Qiao, Changchong Lu, Di Yin, Chen Lin, Haoyuan Peng, and Bo Ren. Osan: A one-stage alignment network to unify multimodal alignment and unsupervised domain adaptation. In *Proceedings of the IEEE/CVF Conference on Computer Vision and Pattern Recognition*, pages 3551–3560, 2023. 1

- [44] Yue Liu, Yunjie Tian, Yuzhong Zhao, Hongtian Yu, Lingxi Xie, Yaowei Wang, Qixiang Ye, and Yunfan Liu. Vmamba: Visual state space model. *arXiv preprint arXiv:2401.10166*, 2024. [2](#), [4](#), [5](#), [6](#), [7](#), [8](#), [11](#), [12](#), [20](#)
- [45] Shaocong Long, Qianyu Zhou, Chenhao Ying, Lizhuang Ma, and Yuan Luo. Diverse target and contribution scheduling for domain generalization. *arXiv preprint arXiv:2309.16460*, 2023. [1](#), [4](#)
- [46] Shaocong Long, Qianyu Zhou, Chenhao Ying, Lizhuang Ma, and Yuan Luo. Rethinking domain generalization: Discriminability and generalizability. *arXiv preprint arXiv:2309.16483*, 2023. [1](#), [19](#)
- [47] Divyat Mahajan, Shruti Tople, and Amit Sharma. Domain generalization using causal matching. In *International Conference on Machine Learning*, pages 7313–7324. PMLR, 2021. [1](#), [4](#)
- [48] Jonathan Munro and Dima Damen. Multi-modal domain adaptation for fine-grained action recognition. In *Proceedings of the IEEE/CVF conference on computer vision and pattern recognition*, pages 122–132, 2020. [1](#)
- [49] Hyeonseob Nam, HyunJae Lee, Jongchan Park, Wonjun Yoon, and Donggeun Yoo. Reducing domain gap by reducing style bias. In *Proceedings of the IEEE/CVF Conference on Computer Vision and Pattern Recognition*, pages 8690–8699, 2021. [8](#), [9](#), [10](#), [20](#)
- [50] Mehrdad Noori, Milad Cheraghlikhani, Ali Bahri, Gustavo A Vargas Hakim, David Osowiechi, Ismail Ben Ayed, and Christian Desrosiers. Tfs-vit: Token-level feature stylization for domain generalization. *Pattern Recognition*, 149:110213, 2024. [2](#), [4](#)
- [51] Namuk Park and Songkuk Kim. How do vision transformers work? *arXiv preprint arXiv:2202.06709*, 2022. [2](#)
- [52] Xingchao Peng, Qinxun Bai, Xide Xia, Zijun Huang, Kate Saenko, and Bo Wang. Moment matching for multi-source domain adaptation. In *Proceedings of the IEEE/CVF International Conference on Computer Vision*, pages 1406–1415, 2019. [8](#), [10](#), [19](#)
- [53] Ronan Perry, Julius Von Kügelgen, and Bernhard Schölkopf. Causal discovery in heterogeneous environments under the sparse mechanism shift hypothesis. *Advances in Neural Information Processing Systems*, 35:10904–10917, 2022. [1](#)
- [54] Fan Qi, Xiaoshan Yang, and Changsheng Xu. A unified framework for multimodal domain adaptation. In *Proceedings of the 26th ACM international conference on Multimedia*, pages 429–437, 2018. [1](#)
- [55] Shiori Sagawa, Pang Wei Koh, Tatsunori B Hashimoto, and Percy Liang. Distributionally robust neural networks. In *International Conference on Learning Representations*, 2019. [8](#), [9](#), [10](#)
- [56] Bernhard Schölkopf, Francesco Locatello, Stefan Bauer, Nan Rosemary Ke, Nal Kalchbrenner, Anirudh Goyal, and Yoshua Bengio. Towards Causal Representation Learning. *arXiv:2102.11107 [cs]*, 2021. [1](#)
- [57] Ramprasaath R Selvaraju, Michael Cogswell, Abhishek Das, Ramakrishna Vedantam, Devi Parikh, and Dhruv Batra. Grad-cam: Visual explanations from deep networks via gradient-based localization. In *Proceedings of the IEEE international conference on computer vision*, pages 618–626, 2017. [7](#), [12](#)
- [58] Shiv Shankar, Vihari Piratla, Soumen Chakrabarti, Siddhartha Chaudhuri, Preethi Jyothi, and Sunita Sarawagi. Generalizing across domains via cross-gradient training. In *International Conference on Learning Representations*, 2018. [4](#)
- [59] Yiran Song, Qianyu Zhou, Xiangtai Li, Deng-Ping Fan, Xuequan Lu, and Lizhuang Ma. Ba-sam: Scalable bias-mode attention mask for segment anything model. In *Proceedings of the IEEE/CVF Conference on Computer Vision and Pattern Recognition*, 2024. [1](#)
- [60] Maryam Sultana, Muzammal Naseer, Muhammad Haris Khan, Salman Khan, and Fahad Shahbaz Khan. Self-distilled vision transformer for domain generalization. In *Proceedings of the Asian Conference on Computer Vision*, pages 3068–3085, 2022. [4](#), [8](#), [9](#), [10](#), [20](#)
- [61] Zhaorui Tan, Xi Yang, and Kaizhu Huang. Rethinking multi-domain generalization with a general learning objective. In *Proceedings of the IEEE/CVF Conference on Computer Vision and Pattern Recognition*, 2024. [8](#), [9](#), [10](#), [20](#)
- [62] Laurens Van der Maaten and Geoffrey Hinton. Visualizing data using t-sne. *Journal of machine learning research*, 9(11), 2008. [12](#), [20](#)
- [63] Hemanth Venkateswara, Jose Eusebio, Shayok Chakraborty, and Sethuraman Panchanathan. Deep Hashing Network for Unsupervised Domain Adaptation. In *2017 IEEE Conference on Computer Vision and Pattern Recognition (CVPR)*, pages 5385–5394, 2017. [8](#), [19](#)
- [64] Mengzhu Wang, Jianlong Yuan, Qi Qian, Zhibin Wang, and Hao Li. Semantic data augmentation based distance metric learning for domain generalization. In *Proceedings of the 30th ACM international conference on multimedia*, pages 3214–3223, 2022. [4](#)
- [65] Pengfei Wang, Zhaoxiang Zhang, Zhen Lei, and Lei Zhang. Sharpness-aware gradient matching for domain generalization. In *Proceedings of the IEEE/CVF Conference on Computer Vision and Pattern Recognition*, pages 3769–3778, 2023. [1](#), [8](#), [9](#), [10](#), [20](#)
- [66] Ye Wang, Junyang Chen, Mengzhu Wang, Hao Li, Wei Wang, Houcheng Su, Zhihui Lai, Wei Wang, and Zhenghan Chen. A closer look at classifier in adversarial domain generalization. In *Proceedings of the 31st ACM International Conference on Multimedia*, pages 280–289, 2023. [4](#)
- [67] Yufei Wang, Haoliang Li, Hao Cheng, Bihan Wen, Lap-Pui Chau, and Alex Kot. Variational disentanglement for domain generalization. *Transactions on Machine Learning Research*, 2022. [4](#)



- [68] Zhuo Wang, Zezheng Wang, Zitong Yu, Weihong Deng, Jiahong Li, Tingting Gao, and Zhongyuan Wang. Domain Generalization via Shuffled Style Assembly for Face Anti-Spoofing. *arXiv:2203.05340 [cs]*, 2022. [1](#), [4](#)
- [69] Ziyang Wang, Jian-Qing Zheng, Yichi Zhang, Ge Cui, and Lei Li. Mamba-unet: Unet-like pure visual mamba for medical image segmentation. *arXiv preprint arXiv:2402.05079*, 2024. [4](#)
- [70] Jianzong Wu, Xiangtai Li, Shilin Xu, Haobo Yuan, Henghui Ding, Yibo Yang, Xia Li, Jiangning Zhang, Yunhai Tong, Xudong Jiang, Bernard Ghanem, and Dacheng Tao. Towards open vocabulary learning: A survey. *T-PAMI*, 2024. [1](#)
- [71] Renkai Wu, Yinghao Liu, Pengchen Liang, and Qing Chang. H-vmunet: High-order vision mamba unet for medical image segmentation. *arXiv preprint arXiv:2403.13642*, 2024. [4](#)
- [72] Yao Xiao, Ziyi Tang, Pengxu Wei, Cong Liu, and Liang Lin. Masked images are counterfactual samples for robust fine-tuning. In *Proceedings of the IEEE/CVF Conference on Computer Vision and Pattern Recognition*, pages 20301–20310, 2023. [1](#), [7](#)
- [73] Qinwei Xu, Ruipeng Zhang, Ya Zhang, Yanfeng Wang, and Qi Tian. A fourier-based framework for domain generalization. In *Proceedings of the IEEE/CVF Conference on Computer Vision and Pattern Recognition*, pages 14383–14392, 2021. [4](#)
- [74] Xufeng Yao, Yang Bai, Xinyun Zhang, Yuechen Zhang, Qi Sun, Ran Chen, Ruiyu Li, and Bei Yu. Pcl: Proxy-based contrastive learning for domain generalization. In *Proceedings of the IEEE/CVF Conference on Computer Vision and Pattern Recognition*, pages 7097–7107, 2022. [4](#), [8](#), [9](#), [10](#), [20](#)
- [75] Chongzhi Zhang, Mingyuan Zhang, Shanghang Zhang, Daisheng Jin, Qiang Zhou, Zhongang Cai, Haiyu Zhao, Xianglong Liu, and Ziwei Liu. Delving deep into the generalization of vision transformers under distribution shifts. In *Proceedings of the IEEE/CVF conference on Computer Vision and Pattern Recognition*, pages 7277–7286, 2022. [4](#)
- [76] Hanlin Zhang, Yi-Fan Zhang, Weiyang Liu, Adrian Weller, Bernhard Schölkopf, and Eric P Xing. Towards principled disentanglement for domain generalization. In *Proceedings of the IEEE/CVF Conference on Computer Vision and Pattern Recognition*, pages 8024–8034, 2022. [4](#)
- [77] Jiangning Zhang, Xiangtai Li, Jian Li, Liang Liu, Zhucun Xue, Boshen Zhang, Zhengkai Jiang, Tianxin Huang, Yabiao Wang, and Chengjie Wang. Rethinking mobile block for efficient attention-based models. In *ICCV*, 2023. [1](#)
- [78] Jiangning Zhang, Xiangtai Li, Guanzhong Tian, Zhucun Xue, Yong Liu, Guansong Pang, and Dacheng Tao. Learning feature inversion for multi-class unsupervised anomaly detection under general-purpose coco-ad benchmark. *arXiv*, 2024. [1](#)
- [79] Marvin Zhang, Henrik Marklund, Nikita Dhawan, Abhishek Gupta, Sergey Levine, and Chelsea Finn. Adaptive risk minimization: Learning to adapt to domain shift. *Advances in Neural Information Processing Systems*, 34:23664–23678, 2021. [8](#), [9](#), [10](#), [20](#)
- [80] Tao Zhang, Xiangtai Li, Haobo Yuan, Shunping Ji, and Shuicheng Yan. Point cloud mamba: Point cloud learning via state space model. *arXiv preprint arXiv:2403.00762*, 2024. [4](#), [6](#), [7](#)
- [81] Yifan Zhang, Xue Wang, Kexin Jin, Kun Yuan, Zhang Zhang, Liang Wang, Rong Jin, and Tieniu Tan. Adanpc: Exploring non-parametric classifier for test-time adaptation. In *International Conference on Machine Learning*, pages 41647–41676. PMLR, 2023. [1](#), [19](#)
- [82] YiFan Zhang, xue wang, Jian Liang, Zhang Zhang, Liang Wang, Rong Jin, and Tieniu Tan. Free lunch for domain adversarial training: Environment label smoothing. In *The Eleventh International Conference on Learning Representations*, 2023. [4](#), [19](#)
- [83] Yi-Fan Zhang, Jindong Wang, Jian Liang, Zhang Zhang, Baosheng Yu, Liang Wang, Dacheng Tao, and Xing Xie. Domain-specific risk minimization for domain generalization. In *Proceedings of the 29th ACM SIGKDD Conference on Knowledge Discovery and Data Mining*, page 3409–3421. Association for Computing Machinery, 2023. [4](#)
- [84] Shanshan Zhao, Mingming Gong, Tongliang Liu, Huan Fu, and Dacheng Tao. Domain Generalization via Entropy Regularization. In *Advances in Neural Information Processing Systems*, volume 33, pages 16096–16107. Curran Associates, Inc., 2020. [1](#), [4](#)
- [85] Yuyang Zhao, Zhun Zhong, Fengxiang Yang, Zhiming Luo, Yaojin Lin, Shaozi Li, and Nicu Sebe. Learning to generalize unseen domains via memory-based multi-source meta-learning for person re-identification. In *Proceedings of the IEEE/CVF conference on computer vision and pattern recognition*, pages 6277–6286, 2021. [4](#)
- [86] Yuyang Zhao, Zhun Zhong, Na Zhao, Nicu Sebe, and Gim Hee Lee. Style-hallucinated dual consistency learning: A unified framework for visual domain generalization. *International Journal of Computer Vision*, pages 1–17, 2023. [1](#)
- [87] Yuyang Zhao, Zhun Zhong, Na Zhao, Nicu Sebe, and Gim Hee Lee. Style-hallucinated dual consistency learning: A unified framework for visual domain generalization. *International Journal of Computer Vision*, 132(3):837–853, 2024. [1](#)
- [88] Zangwei Zheng, Xiangyu Yue, Kai Wang, and Yang You. Prompt vision transformer for domain generalization. *arXiv preprint arXiv:2208.08914*, 2022. [2](#)

- [89] Kaiyang Zhou, Ziwei Liu, Yu Qiao, Tao Xiang, and Chen Change Loy. Domain generalization: A survey. *IEEE Transactions on Pattern Analysis and Machine Intelligence*, 45(4):4396–4415, 2022. [1](#)
- [90] Kaiyang Zhou, Yongxin Yang, Timothy Hospedales, and Tao Xiang. Learning to generate novel domains for domain generalization. In *European conference on computer vision*, pages 561–578. Springer, 2020. [4](#)
- [91] Kaiyang Zhou, Yongxin Yang, Yu Qiao, and Tao Xiang. Domain generalization with mixstyle. In *International Conference on Learning Representations*, 2021. [8](#), [9](#), [10](#), [20](#)
- [92] Kaiyang Zhou, Yongxin Yang, Yu Qiao, and Tao Xiang. Mixstyle neural networks for domain generalization and adaptation. *International Journal of Computer Vision*, 132(3):822–836, 2024. [1](#), [4](#), [19](#)
- [93] Qianyu Zhou, Zhengyang Feng, Qiqi Gu, Guangliang Cheng, Xuequan Lu, Jianping Shi, and Lizhuang Ma. Uncertainty-aware consistency regularization for cross-domain semantic segmentation. *Computer Vision and Image Understanding*, 221:103448, 2022. [1](#)
- [94] Qianyu Zhou, Zhengyang Feng, Qiqi Gu, Jiangmiao Pang, Guangliang Cheng, Xuequan Lu, Jianping Shi, and Lizhuang Ma. Context-aware mixup for domain adaptive semantic segmentation. *IEEE Transactions on Circuits and Systems for Video Technology*, 33(2):804–817, 2023. [1](#)
- [95] Qianyu Zhou, Qiqi Gu, Jiangmiao Pang, Xuequan Lu, and Lizhuang Ma. Self-adversarial disentangling for specific domain adaptation. *IEEE Transactions on Pattern Analysis and Machine Intelligence*, 45(7):8954–8968, 2023. [1](#)
- [96] Qianyu Zhou, Xiangtai Li, Lu He, Yibo Yang, Guangliang Cheng, Yunhai Tong, Lizhuang Ma, and Dacheng Tao. Transvod: end-to-end video object detection with spatial-temporal transformers. *IEEE Transactions on Pattern Analysis and Machine Intelligence*, 45(6):7853–7869, 2023. [1](#)
- [97] Qianyu Zhou, Ke-Yue Zhang, Taiping Yao, Xuequan Lu, Shouhong Ding, and Lizhuang Ma. Test-time domain generalization for face anti-spoofing. In *Proceedings of the IEEE/CVF Conference on Computer Vision and Pattern Recognition*, 2024. [1](#)
- [98] Qianyu Zhou, Ke-Yue Zhang, Taiping Yao, Xuequan Lu, Ran Yi, Shouhong Ding, and Lizhuang Ma. Instance-aware domain generalization for face anti-spoofing. In *Proceedings of the IEEE/CVF Conference on Computer Vision and Pattern Recognition*, pages 20453–20463, 2023. [1](#)
- [99] Qianyu Zhou, Ke-Yue Zhang, Taiping Yao, Ran Yi, Shouhong Ding, and Lizhuang Ma. Adaptive mixture of experts learning for generalizable face anti-spoofing. In *Proceedings of the 30th ACM International Conference on Multimedia*, pages 6009–6018, 2022. [1](#)
- [100] Qianyu Zhou, Chuyun Zhuang, Ran Yi, Xuequan Lu, and Lizhuang Ma. Domain adaptive semantic segmentation via regional contrastive consistency regularization. In *IEEE International Conference on Multimedia and Expo*, pages 01–06, 2022. [1](#)
- [101] Lianghai Zhu, Bencheng Liao, Qian Zhang, Xinlong Wang, Wenyu Liu, and Xinggang Wang. Vision mamba: Efficient visual representation learning with bidirectional state space model. *arXiv preprint arXiv:2401.09417*, 2024. [2](#), [4](#), [5](#), [7](#)

## A Supplementary Material

### A.1 Experiment Details

**Dataset Details.** In this section, we provide details of the 5 commonly used DG benchmarks in Table 10. The data in these datasets originates from various sources with distinct characteristics, such as hand-drawn illustrations, software-composited images, object-centered photographs, and scene-centered shots.

**Evaluation Protocols.** Following the standard evaluation protocols [20, 92, 7, 81, 46], we report the generalization performance based on the train-domain validation, *i.e.*, selecting one domain as the target domain and training on the remaining domains. Each source domain is split with an 80%/20% train/validation ratio. The validation parts from these source domains collectively constitute the validation set used for the model evaluation.

**Hyperparameters for DomainNet.** The benchmark DomainNet [52] presents a great challenge, containing 586575 images. Training 10,000 iterations represents less than two complete epochs on DomainNet, which is insufficient for the model to converge effectively. Consequently, recent state-of-the-art DG works [7, 35, 82] increase the iterations to 15000 with a batch size of 32 for each domain. To make a fair comparison while considering the constraints posed by GPU, our proposed DGMamba undergoes 80000 iterations with a batch size of 6 for each source domain. The corresponding initial learning rate is searched in [7e-4, 8.5e-4].

Table 10: Statistics of DG benchmarks.

Dataset	Domain	# image	# image	# class
PACS [36]	Art	2048	9991	7
	Photo	1670		
	Clipart	2344		
	Sketch	3929		
VLCS [14]	Caltech	1415	10729	5
	LabelMe	2656		
	SUN	3282		
	PASCAL	3376		
OfficeHome [63]	Art	2427	15588	65
	Clipart	4365		
	Product	4439		
	Real	4357		
TerraIncognita [4]	L100	4741	24330	10
	L38	9736		
	L43	3970		
	L46	5883		
DomainNet [52]	Clipart	48129	586575	345
	Infograph	51605		
	Painting	72266		
	Quickdraw	172500		
	Real	172947		
	Sketch	69128		

Table 11: Comparison of state-of-the-art DG methods with our DGMamba. Out-of-domain generalization performance on five commonly used benchmarks is reported. The best results are bolded.

Method	Backbone	Venue	Dataset					Avg.(↑)
			PACS	VLCS	OfficeHome	TerraIncognita	DomainNet	
VREx [34]	ResNet50	ICML'2021	84.9	78.3	66.4	46.4	33.6	61.9
RSC [29]	ResNet50	ECCV'2020	85.2	77.1	65.5	46.6	38.9	62.7
MTL [6]	ResNet50	JMLR'2021	84.6	77.2	66.4	45.6	40.6	62.9
Mixstyle [91]	ResNet50	ICLR'2021	85.2	77.9	60.4	44.0	34.0	60.3
SagNet [49]	ResNet50	CVPR'2021	86.3	77.8	68.1	48.6	40.3	64.2
ARM [79]	ResNet50	NeurIPS'2021	85.1	77.6	64.8	45.5	35.5	61.7
SWAD [7]	ResNet50	NeurIPS'2021	88.1	79.1	70.6	50.0	46.5	66.9
PCL [74]	ResNet50	CVPR'2022	88.7	78.0	71.6	52.1	47.7	67.6
SAGM [65]	ResNet50	CVPR'2023	86.6	80.0	70.1	48.8	45.0	66.1
iDAG [30]	ResNet50	ICCV'2023	88.8	76.9	71.8	46.1	47.7	66.3
GMDG [61]	ResNet50	CVPR'2024	85.6	79.2	70.7	50.1	44.6	66.0
SDViT [60]	DeiT-S	ACCV'2022	86.3	78.9	71.5	44.3	45.8	65.4
GMoE [35]	DeiT-S	ICLR'2023	86.7	78.0	72.4	45.6	48.3	66.2
DGMamba	VMamba-T	Ours	<b>91.2</b>	<b>80.8</b>	<b>77.0</b>	<b>54.6</b>	<b>49.6</b>	<b>70.6</b>

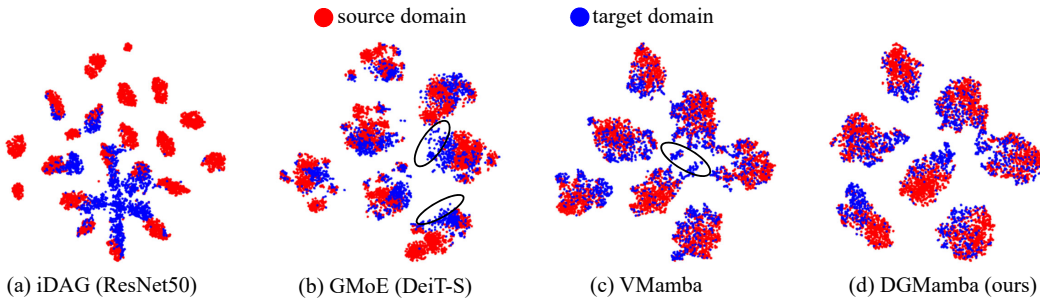


Figure 7: Visualizations with t-SNE embeddings [62] illustrating features’ distribution gaps between the source and target domains generated by (a) iDAG [30], (b) GMoE [35], (c) VMamba [44], and (d) DGMamba (ours), respectively. Our proposed DGMamba displays the superior feature alignment.

**Overall Architecture.** For an input image  $x$ , it undergoes initial processing into patches  $x_i \in x$  utilizing a convolution neural network with layer normalization. These patches are subsequently scanned to be processed by four Mamba blocks. Down-sampling is applied after the first three Mamba blocks to generate feature maps with different resolutions. Finally, prediction is performed using a linear classifier subsequent to the layer normalization, average pooling, and flattening operations.

## A.2 Additional Experiments

**Comparison across Five Benchmarks.** In Table 11, we present a summary of the generalization performance results across five DG benchmarks with training-validation selection. Notably, our proposed DGMamba remarkably outperforms the state-of-the-art DG approaches across all benchmarks, yielding an average gain of 4.4%. The significant enhancements across diverse scenarios from different benchmarks underscore the excellent ability of our DGMamba to tackle distribution shifts.

**Visualization for Distribution Gaps.** To visually demonstrate that our proposed DGMamba could effectively address the distribution shifts between diverse domains, we employ the t-SNE technique [62] to examine the representation’s distribution gaps across domains. We conduct experiments on PACS with ‘Art’ as the target domain. Figure 7 presents the visualization results based on the CNN-based method iDAG [30], ViT-based method GMoE [35], VMamba [44], and our proposed DGMamba, respectively. Notably, our DGMamba demonstrates a reduced distribution gap between the source and target domains compared to these state-of-the-art methods, indicating its superiority in learning domain-invariant features. In contrast, the representation generated by iDAG exhibits a noticeable distinction between the source and target domains, indicating its weakness in tackling distribution shifts. For GMoE, there exist target features that are away from the source features, as indicated by the

Table 12: Comparison of state-of-the-art DG methods with our DGMamba with diverse backbones. The best results are bolded.

Method	Backbone	Params.	Target domain				Avg.(↑)
			Art	Cartoon	Photo	Sketch	
iDAG [30] (ICCV'2023)	ResNet50	25M	90.8	83.7	98.0	82.7	88.8
iDAG [30] (ICCV'2023)	ResNet101	43M	89.0	84.9	98.3	84.7	89.2
GMoE [35] (ICLR'2023)	DeiT-S	34M	89.4	83.9	99.1	74.5	86.7
GMoE [35] (ICLR'2023)	DeiT-B	133M	91.0	84.0	99.3	82.7	89.2
DGMamba (ours)	VMamba-T	31M	91.3	87.0	99.0	87.3	91.2
DGMamba (ours)	VMamba-S	49M	94.1	87.8	99.6	<b>89.0</b>	92.6
DGMamba (ours)	VMamba-B	88M	<b>95.1</b>	<b>89.2</b>	<b>99.8</b>	87.9	93.0

black circles. Besides, the representations produced by GMoE exhibit poor intra-class compactness. For VMamba, the ability to align features is inferior to our DGMamba, manifesting by the distant target features marked by the black circle, and the distinction between classes is not as clear as that in DGMamba.

**Performance with Diverse Backbones.** To fully unleash the potential of our proposed DGMamba, we investigate the impact of utilizing larger backbones, *i.e.*, stacking more Mamba layers or increasing the embedding dimension to facilitate capturing genuine features. Specifically, we conduct experiments on PACS utilizing VMamba-S and VMamba-B. VMamba-S comprises 4 blocks, each including 2, 2, 15, and 2 Mamba layers, with an embedding dimension of 96. VMamba-B maintains the same Mamba blocks and layers as VMamba-S, with an increased embedding dimension of 128. The generalization performances are concluded in Table 12, demonstrating that deeper Mamba architectures or larger embedding dimensions could enhance the model generalizability. Furthermore, our proposed DGMamba demonstrates superior generalization performance compared to CNN-based or ViT-based models, while maintaining comparable or fewer parameters. These results underscore the effectiveness of DGMamba in mitigating domain shifts.